

Sum-rules for Raman scattering off strongly correlated electron systems

Luca de' Medici,¹ Antoine Georges,² and Gabriel Kotliar³

¹*Department of Physics and Center for Materials Theory, Rutgers University, Piscataway, New Jersey 08854, USA*

²*Centre de Physique Théorique, Ecole Polytechnique, 91128 Palaiseau Cedex, France*

³*Department of Physics and Center for Material Theory, Rutgers University, Piscataway, New Jersey 08854, USA*

(Received 5 March 2008; revised manuscript received 10 May 2008; published 23 June 2008)

We investigate sum-rules applying to the Raman intensity in a strongly correlated system close to the Mott transition. Quite generally, it can be shown that provided the frequency integration is performed up to a cutoff smaller than the upper Hubbard band a sum-rule applies to the nonresonant Raman signal of a doped Mott insulator, resulting in an integrated intensity, which is proportional to the doping level. We provide a detailed derivation of this sum-rule for the t - J model for which the frequency cutoff can be taken to infinity and an unrestricted sum-rule applies. A quantitative analysis of the sum-rule is also presented for the d -wave superconducting phase of the t - J model, using slave-boson methods. The case of the Hubbard model is studied in the framework of dynamical mean-field theory, with special attention to the cut-off dependence of the restricted sum-rule and also to the intermediate coupling regime. The sum-rule investigated here is shown to be consistent with recent experimental data on cuprate superconductors, reporting measurements of Raman scattering intensities on an absolute scale.

DOI: [10.1103/PhysRevB.77.245128](https://doi.org/10.1103/PhysRevB.77.245128)

PACS number(s): 71.27.+a, 74.72.-h, 78.30.-j

I. INTRODUCTION

Restricted sum-rules (relating the partial integral of the intensity up to a cutoff with a correlation function) are useful tools for analyzing spectroscopic information in strongly correlated materials. For example the sum-rule for the optical conductivity has received a lot of attention in the context of cuprates.¹⁻⁵

In contrast the sum-rules for the Raman scattering intensity have been less studied. These were first considered in Refs. 6 and 7. Recently, it has been stressed that for a doped Mott insulator the nonresonant Raman intensity should be proportional to doping^{8,9} provided the frequency integration is carried up to a cutoff which is such that contributions from the upper Hubbard band are not included. This proved instrumental in analyzing recent experiments on cuprate superconductors⁹ that revived the debate about the relationship between the pseudogap and the superconductive gap in the underdoped phase of these compounds.¹⁰⁻¹³

The goal of this paper is to analyze the Raman sum-rules and their dependence on the strength of the interactions, doping, temperature, and choice of upper cutoff.

In Sec. III we show that for the t - J model the right-hand side that enters the sum-rule for Raman scattering is proportional to doping. In this case, the frequency cutoff can be taken to infinity (since the upper Hubbard band is absent due to the constraint of no-double-occupancy), hence making a rigorous theoretical analysis easier.

We then evaluate explicitly the Raman response function of a doped Mott insulator by solving the Hubbard model using dynamical mean-field theory (DMFT). We explore the region in which the Raman intensity scales with doping, and how this region varies with the cutoff used in the sum-rule, and contrast those results with that of a correlated material slightly below the Mott transition. In Sec. V we compare the results of our calculation, for different choices of the upper cutoff, with experimental data and then in Sec. VI we con-

clude with predictions for the temperature dependence of the integrated low-energy Raman intensity using a slave-bosons treatment of the t - J model.

II. RAMAN SUM-RULES

Raman scattering is a photon-in photon-out process happening when an external electromagnetic field is applied on a system, and its nonresonant cross section can be calculated from the Fermi's golden rule, reading;

$$R(\mathbf{q}, \Omega) = 2\pi \sum_{i,f} \frac{\exp(-\beta \varepsilon_i)}{\mathcal{Z}} \left| g(\mathbf{k}_i) g(\mathbf{k}_f) \sum_{rs} e_r^i e_s^f \langle f | \tau^{rs}(\mathbf{q}) | i \rangle \right|^2 \times \delta(\varepsilon_f - \varepsilon_i - \Omega), \quad (1)$$

where β is the inverse temperature, $g(\mathbf{q}) = (hc^2/V\omega_q)^{1/2}$, where V is the volume, ω_q and \hat{e} are energy and polarization vectors of the photons (i, f indicate initial and final states of the process), and

$$\tau^{rs}(\mathbf{q}) = \sum_{\mathbf{k}} \frac{\partial^2 \epsilon_{\mathbf{k}}}{\partial k_r \partial k_s} c_{\mathbf{k}+\mathbf{q}/2, \sigma}^\dagger c_{\mathbf{k}-\mathbf{q}/2, \sigma} \quad (2)$$

is the stress operator tensor. $\varepsilon_{i,f}$ is the energy of the initial or final state of the system, Ω is the transferred energy, $c_{\mathbf{k}}^\dagger$ creates an electron of momentum \mathbf{k} , $\epsilon_{\mathbf{k}}$ is the one-electron dispersion of the model under consideration, and r, s are Cartesian components.

Then by the fluctuation-dissipation theorem, the scattering intensity in one channel,

$$I_{rs}(\mathbf{q}, \Omega) = \sum_{i,f} \frac{\exp(-\beta \varepsilon_i)}{\mathcal{Z}} |\langle f | \tau^{rs}(\mathbf{q}) | i \rangle|^2 \delta(\varepsilon_f - \varepsilon_i - \Omega) = \frac{\chi''_{rs}(\mathbf{q}, \Omega)}{1 - e^{-\beta \Omega}} \quad (3)$$

is related to the imaginary part of a response function, i.e.,

$$\chi_{rs}(\mathbf{q}, t) = i\Theta(t)\langle[\tau^{rs}(\mathbf{q}, t), \tau^{rs}(0, 0)]\rangle, \quad (4)$$

which is a stress-stress correlation function of the unperturbed system.

We will consider in the following only the $\mathbf{q}=0$ contribution, since the photon momentum is always much smaller than the Fermi momentum.

What is remarkable in Raman scattering¹⁴ is that by tuning the polarization of the incident and of the detected outgoing photons one can exploit selection rules to sort out different processes in the probed material. This is of particular utility in order to separate the response due to electronic excitations in different areas of the Brillouin zone, thus, allowing to probe k -dependent properties of the material.

This is, in particular, a key issue for the physics of cuprates in which nodal and antinodal regions of the Brillouin zone are known to behave in distinctly different manners. It is remarkable that despite being a $q=0$ probe (as is optics) Raman scattering can still address momentum-selective issues by exploiting the dependence of the Raman vertex on the polarization of the incident and scattered light. Especially for a material with perfect in-plane equivalence of the a - and b -axis, the B_{2g} and B_{1g} geometry mainly probe, respectively, the nodal and antinodal regions.

In the nonresonant response, by choosing the direction of the polarizations e^i, e^f , one isolates contributions by the different elements $\tau^{rs}(\mathbf{q})$ of the stress tensor.

As an example, let's consider a square lattice with nearest-neighbor and next-nearest-neighbor hoppings t and t' that give rise to the dispersion in k space,

$$\epsilon_{\mathbf{k}} = -2t(\cos k_x + \cos k_y) + 4t' \cos k_x \cos k_y. \quad (5)$$

Then, in the B_{2g} scattering geometry, e^i, e^f are perpendicular between each other and parallel to the x - y plane axes, and the Raman scattering operator is $\tau^{xy}(\mathbf{q})$. From Eq. (2) one then sees that the sum over the momentum space is weighted by the vertex factor,

$$\frac{\partial^2 \epsilon_{\mathbf{k}}}{\partial k_x \partial k_y} = 4t' \sin k_x \sin k_y, \quad (6)$$

thus, sorting out the contribution along the nodal directions.

Analogously, one can show how in the B_{1g} geometry, with e^i, e^f perpendicular but oriented along the lattice diagonals, one selects the antinodal directions in k space.

In this work we are interested in discussing the sum-rules fulfilled by the Raman B_{2g} nonresonant response. It is well known^{7,15} that any susceptibility of the general Kubo form [Eq. (4)] fulfills the following sum-rule:

$$\frac{2}{\pi} \int_0^\infty d\Omega \Omega \chi''_{(\mathcal{O}, \mathcal{O})}(\Omega) = \langle[\mathcal{O}, [\mathcal{H}, \mathcal{O}]]\rangle, \quad (7)$$

where \mathcal{O} is the operator to the fluctuations of which the susceptibility is associated.

Hence, for the B_{2g} Raman scattering this sum-rule reads,

$$\frac{2}{\pi} \int_0^\infty d\Omega \Omega \chi''_{B_{2g}}(\Omega) = \langle[[\tau^{xy}, \mathcal{H}], \tau^{xy}]\rangle. \quad (8)$$

Equation (8) has been used in Ref. 9 to normalize the Raman spectra in mercury-based cuprates. In the following we will show that the right-hand side of this sum-rule is proportional to doping in the t - t' - J model.¹⁶

III. B_{2g} RAMAN SUM-RULE IN THE t - t' - J MODEL AND ITS PROPORTIONALITY TO DOPING

In this section we report the analysis of the direct evaluation of the right-hand side of the B_{2g} sum-rule Eq. (8) in the t - t' - J model on the square lattice.

This model is represented by the Hamiltonian,

$$H = \sum_{i,j,\sigma} (t_{ij} c_{i,\sigma}^\dagger c_{j,\sigma} + \text{H.c.}) + \sum_{kl} 4J_{kl} \left(S_k \cdot S_l - \frac{1}{4} n_k n_l \right), \quad (9)$$

acting on the Hilbert space where states with doubly occupied sites have been removed.

Here $c_{i,\sigma}^\dagger$ is the operator that creates an electron with spin σ in a state localized on-site i and t_{ij} is the hopping integral between single-particle states at sites i and j . S_k is the electron spin at site k and $4J_{kl} \geq 0$ is the antiferromagnetic superexchange and is zero for $k=l$ and nonzero at (but not necessarily restricted to) nearest neighbors.

The hopping matrix t_{ij} is chosen to have nonzero elements only for nearest ($t_{ij}=-t$) and next-nearest ($t_{ij}=t'$) neighbors. The on-site element is the chemical potential term that tunes the filling ($t_{ii}=-\mu$). The bare electronic dispersion is given by Eq. (5).

We have to evaluate the doping dependence of the average of the double commutator [Eq. (8)] in this model.

To implement the non-double-occupancy constraint, we use the formalism of the Hubbard Operators. Definitions and some algebra tricks for this formalism can be found in Appendix. We thus obtain an exact expression of the right-hand side of the sum-rule.

Both the stress operator [Eq. (2)] and the Hamiltonian $H=H_t+H_J$ can be readily expressed with these operators $X_{\alpha\beta}$;

$$H_t = \sum_{ij\sigma} t_{ij} X_{\sigma 0}^i X_{0\sigma}^j, \quad (10)$$

$$H_J = \sum_{kl,\alpha\beta} 2J_{kl} (X_{\alpha\beta}^k X_{\beta\alpha}^l - X_{\alpha\alpha}^k X_{\beta\beta}^l), \quad (11)$$

$$\tau^{xy}(0) = \sum_{ij\sigma} \tau_{ij}^{xy} X_{\sigma 0}^i X_{0\sigma}^j, \quad (12)$$

where the stress component τ^{xy} has elements,

$$\tau_{ij}^{xy} = \sum_{\mathbf{k}} e^{i\mathbf{k}\cdot\mathbf{r}_{ij}} \frac{\partial^2 \epsilon_{\mathbf{k}}}{\partial k_x \partial k_y} = 4t' \sum_{\mathbf{k}} \cos(\mathbf{k} \cdot \mathbf{r}_{ij}) \sin k_x \sin k_y \quad (13)$$

that are nonzero only when i and j are next-nearest neighbor, as can be deduced by this expression (in order to lighten the notation we will drop the superscript xy in τ_{ij}^{xy} from now on).

The evaluation of the commutators leads, for the hopping part,¹⁷

$$\begin{aligned}
[[\tau^{xy}, H_t], \tau^{xy}] = & \sum_{abcd, \alpha \neq \beta} [(\tau_{ab} t_{bc} - \tau_{bc} t_{ab}) \tau_{bd} \\
& - (\tau_{ac} t_{cd} - \tau_{cd} t_{ac}) \tau_{bc}] \\
& \times [X_{\alpha 0}^a X_{\beta 0}^b X_{0\alpha}^c X_{0\beta}^d - X_{\alpha 0}^a X_{\beta 0}^b X_{0\beta}^c X_{0\alpha}^d] \\
& + \sum_{abcd, \alpha \beta \sigma} (\tau_{ab} t_{bc} - \tau_{bc} t_{ab}) \tau_{cd} \\
& \times [X_{\alpha 0}^a D_{\sigma\alpha}^b D_{\beta\sigma}^c X_{0\beta}^d \\
& - X_{\beta 0}^d D_{\sigma\beta}^c D_{\alpha\sigma}^b X_{0\alpha}^a], \quad (14)
\end{aligned}$$

where we have defined (see also Appendix) the bosonic operator $D_{\alpha\beta}^i \equiv (X_{\alpha\beta}^i + \delta_{\alpha\beta} X_{00}^i)$. All the other operators in the expression are fermionic.

In the following analysis we will show that the average value of this expression and of the other parts of the double commutator is $\sim \delta$ at the leading order.

Indeed, after having brought together and collapsed all the operators that refer to the same site into one ($X_{\alpha 0}^a X_{0\alpha}^a = X_{\alpha\alpha}^a$, see Appendix), expressions containing X_{00}^i or fermionic operators vanish exactly as $\delta \rightarrow 0$ because of the constraint.

This is an exact statement but it can also be seen more explicitly in approximate schemes like slave-bosons, as we will show here. Indeed one can evaluate the doping dependence of the average of the different terms in the double commutator by considering that each fermionic operator on a different site carries a renormalization factor proportional to $b \sim \sqrt{\delta}$ while an operator X_{00}^i carries a factor $|b^2| \sim \delta$;

$$X_{\alpha\beta}^i = f_{i\alpha}^\dagger f_{i\beta}, X_{\alpha 0}^i = f_{i\alpha}^\dagger b_i, X_{0\alpha}^i = b_i^\dagger f_{i\alpha}, X_{00}^i = b_i^\dagger b_i. \quad (15)$$

One can then evaluate, using these relations, the explicit dependence in doping of each term of the sum corresponding to the right-hand side of Eq. (8) with the prescription of collapsing first the operators living on same sites into one.

We will see that the coefficients of all terms containing no X_{00}^i and less than two fermionic operators on different sites (that we call ‘‘dangerous terms’’) vanish, and thus, the dependence is $\propto \delta$ at the leading order.

Let’s analyze then $[[\tau^{xy}, H_t], \tau^{xy}]$.

For the first of the two four-fermion contributions in Eq. (14), these dangerous terms occur when in the sum $a=c$ and $b=d$. For example, the first product in this case contributes to the sum (over $a \neq b, \alpha \neq \beta$) with terms like,

$$X_{\alpha 0}^a X_{\beta 0}^b X_{0\alpha}^a X_{0\beta}^b = -X_{\alpha\alpha}^a X_{\beta\beta}^b = -f_{a\alpha}^\dagger f_{a\alpha} f_{b\beta}^\dagger f_{b\beta}. \quad (16)$$

Since in this case one can anticommute the Hubbard operators in order to collapse the ones that refer to the same sites ($X_{\alpha 0}^a X_{0\alpha}^a = X_{\alpha\alpha}^a$, see Appendix) and then evaluate the averages using the slave-bosons operatorial equivalences [Eq. (15)].

This term is ‘‘dangerous’’ since its average is not obviously proportional to doping. But, it does not actually contribute to the sum since its coefficient, in this case, vanishes. Indeed, for $a=c$ and $b=d$ its coefficient becomes $(\tau_{ab} t_{ba} - \tau_{ba} t_{ab}) \tau_{bb} - (\tau_{aa} t_{ab} - \tau_{ab} t_{aa}) \tau_{ba} = 0$, since $\tau_{ii} = t_{ii} = 0$.

The second four-fermion product instead is dangerous when $a=d$ and $b=c$ and again its coefficient $(\tau_{ab} t_{bb} - \tau_{bb} t_{ab}) \tau_{ba} - (\tau_{ab} t_{ba} - \tau_{ba} t_{ab}) \tau_{bb} = 0$.

The two-fermion terms are dangerous when $a=d$ and the coefficient becomes $(\tau_{ab} t_{bc} - \tau_{bc} t_{ab}) \tau_{ca}$. For this to be nonzero a and c have to be next-nearest neighbors. Then, it is easy to see that on the cubic lattice (and within the ranges previously defined for the matrices t_{ij} and τ_{ij}) it is impossible to chose the site b such that the coefficient is nonzero.

Thus, we have shown that all contributions of $[[\tau^{xy}, H_t], \tau^{xy}]$ with a less than linear dependence in doping vanish.

For the magnetic part of the Hamiltonian one has,

$$\begin{aligned}
[[\tau^{xy}, H_J], \tau^{xy}] = & \sum_{abcd, \alpha \neq \beta} 4\tau_{ab} \tau_{cd} (J_{bc} - J_{ac} - J_{bd} + J_{ad}) \\
& \times (X_{\alpha 0}^a X_{0\beta}^b X_{\beta 0}^c X_{0\alpha}^d - X_{\alpha 0}^a X_{0\alpha}^b X_{\beta 0}^c X_{0\beta}^d) \\
& + \sum_{abcd, \sigma\alpha \neq \beta} 2\tau_{ab} \tau_{bd} (J_{bc} - J_{ac}) [X_{\alpha 0}^a D_{\sigma\beta}^b X_{0\sigma}^d X_{\beta\alpha}^c \\
& + X_{\alpha\beta}^c X_{\beta 0}^a D_{\sigma\alpha}^b X_{0\sigma}^d + X_{\sigma 0}^d D_{\alpha\sigma}^b X_{\alpha\beta}^c X_{\beta\alpha}^c \\
& + X_{\alpha\beta}^c X_{\sigma 0}^d D_{\beta\sigma}^b X_{0\alpha}^a - X_{\alpha 0}^a D_{\sigma\alpha}^b X_{0\sigma}^d X_{\beta\beta}^c \\
& - X_{\beta\beta}^c X_{\alpha 0}^a D_{\sigma\alpha}^b X_{0\sigma}^d - X_{\sigma 0}^d D_{\alpha\sigma}^b X_{0\alpha}^a X_{\beta\beta}^c \\
& - X_{\beta\beta}^c X_{\sigma 0}^d D_{\alpha\sigma}^b X_{0\alpha}^a]. \quad (17)
\end{aligned}$$

The first of the four-fermion terms is never dangerous, since even when $a=d$ and $b=c$, the product $X_{0\beta}^b X_{\beta 0}^c = X_{00}^b$, and thus, its average is proportional to doping.

The second of the four-fermion terms is dangerous when $a=b$ and $c=d$. However, in these configurations the coefficient becomes $2\tau_{aa} \tau_{cc} (J_{ac} - J_{ac} - J_{ac} + J_{ac}) = 0$.

The analysis of the two-fermion terms is a little more involved. They are dangerous when $a=d$. The product in this case becomes [in $D_{\alpha\beta}^i \equiv (X_{\alpha\beta}^i + \delta_{\alpha\beta} X_{00}^i)$ we can drop the X_{00} operators¹⁸]

$$\begin{aligned}
& X_{\alpha\sigma}^a X_{\sigma\beta}^b X_{\beta\alpha}^c + X_{\alpha\beta}^c X_{\sigma\alpha}^b X_{\beta\sigma}^a + X_{\sigma\beta}^c X_{\alpha\sigma}^b X_{\beta\alpha}^c + X_{\alpha\beta}^c X_{\beta\sigma}^b X_{\sigma\alpha}^a \\
& - X_{\alpha\sigma}^a X_{\sigma\alpha}^b X_{\beta\beta}^c - X_{\beta\beta}^c X_{\sigma\alpha}^b X_{\beta\sigma}^a - X_{\sigma\alpha}^b X_{\alpha\sigma}^c X_{\beta\beta}^c - X_{\beta\beta}^c X_{\alpha\sigma}^b X_{\sigma\alpha}^a.
\end{aligned}$$

We used the fact that operators at sites a and d always commute with operators at site b since the coefficient vanishes when $a=b$ or $d=b$.

We then have to exchange the indices a and b in the III, IV, VII, and VIII term in order to match the spin indices with the remaining four terms (the operators in a and b commute). We obtain

$$\begin{aligned}
& X_{\alpha\sigma}^a X_{\sigma\beta}^b X_{\beta\alpha}^c + X_{\alpha\beta}^c X_{\sigma\alpha}^b X_{\beta\sigma}^a - X_{\alpha\sigma}^a X_{\sigma\beta}^b X_{\beta\alpha}^c \\
& - X_{\alpha\beta}^c X_{\sigma\alpha}^b X_{\beta\sigma}^a - X_{\alpha\sigma}^a X_{\sigma\alpha}^b X_{\beta\beta}^c - X_{\beta\beta}^c X_{\sigma\alpha}^b X_{\beta\sigma}^a \\
& + X_{\alpha\sigma}^a X_{\sigma\alpha}^b X_{\beta\beta}^c + X_{\beta\beta}^c X_{\sigma\alpha}^b X_{\beta\sigma}^a = 0,
\end{aligned}$$

since the renaming of a and b changes the sign of the coefficient $\tau_{ab} \tau_{bd} (J_{bc} - J_{ac})$. Thus, the terms cancel two by two (I and III, II and IV, V and VII, and VI and VIII).

We can then conclude that all the terms that contribute to $\langle [[\tau^{xy}, H], \tau^{xy}] \rangle$ are at least $\propto \delta$ and that the sum-rule integral [Eq. (8)] is proportional to doping. Note that this is true *irrespective of the nature of the possible long-range ordering* (e.g., both in the normal and superconducting states).

IV. DYNAMICAL MEAN-FIELD THEORY CALCULATION IN THE HUBBARD MODEL

In this section we report the explicit calculation of the Raman response function for the doped Hubbard model,

$$H = \sum_{ij,\sigma} t_{ij}(c_{i\sigma}^\dagger c_{j\sigma} + \text{H.c.}) + U \sum_i n_{i\uparrow} n_{i\downarrow}, \quad (18)$$

at strong and intermediate coupling within DMFT (Ref. 19). One of our main motivations for studying the Hubbard model is to investigate the *restricted* sum-rule up to a frequency cutoff Ω_c and study the dependence on the cutoff frequency.

Single-site DMFT freezes spatial fluctuations while fully retaining the local dynamics. It thus allows to calculate dynamical response functions in the local self-energy approximation.²⁰

Since the Raman vertex is odd under, e.g., $k_x \rightarrow -k_x$, vertex corrections vanish in the local self-energy approximation¹⁹ and the stress-stress response function Eq. (4) at $\mathbf{q}=0$ reduces to the simple bubble diagram of dressed propagators, which reads (in the imaginary time formalism),

$$\chi(i\Omega) = \frac{1}{\beta} \sum_{\mathbf{k}, i\nu} \left(\frac{\partial^2 \epsilon_{\mathbf{k}}}{\partial k_x \partial k_y} \right)^2 G(\mathbf{k}, i\nu) G(\mathbf{k}, i\nu + i\Omega), \quad (19)$$

and analytically continued,

$$\chi''(\Omega) = \int d\epsilon V(\epsilon) \int d\omega A(\epsilon, \omega) A(\epsilon, \omega + \Omega) [f(\omega) - f(\omega + \Omega)], \quad (20)$$

where

$$\begin{aligned} V(\epsilon) &= \sum_{\mathbf{k}} \left(\frac{\partial^2 \epsilon_{\mathbf{k}}}{\partial k_x \partial k_y} \right)^2 \delta(\epsilon - \epsilon_{\mathbf{k}}) \\ &= (4t')^2 \sum_{\mathbf{k}} \sin^2 k_x \sin^2 k_y \delta(\epsilon - \epsilon_{\mathbf{k}}) \end{aligned} \quad (21)$$

is the appropriate form factor obtained by summing over \mathbf{k} the product of two B_{2g} geometry vertices [Eq. (6)]. It can be calculated once and for all and for the dispersion, [Eq. (5)] is a smooth function. $A(\epsilon, \omega)$ is the spectral function,

$$\begin{aligned} A(\mathbf{k}, \omega) &= -\frac{1}{\pi} \text{Im} G(\mathbf{k}, \omega) \\ &= -\frac{1}{\pi} \frac{\text{Im} \Sigma(\omega)}{(\omega + \mu - \epsilon_{\mathbf{k}} - \text{Re} \Sigma(\omega))^2 + (\text{Im} \Sigma(\omega))^2}, \end{aligned} \quad (22)$$

for $\epsilon_{\mathbf{k}} = \epsilon$ and is easily accessible in single-site DMFT²¹ through the knowledge of the local self-energy.²²

Hence, in this approximation the nonresonant Raman response is readily calculated by convoluting two single-particle spectral functions with the appropriate kernel $V(\epsilon)$.

We have solved the Hubbard model with DMFT at zero temperature and finite doping for $U/W=2.5$ (W is the bandwidth), which can be seen as a rather strong coupling, and for an intermediate coupling $U/W=1.35$.

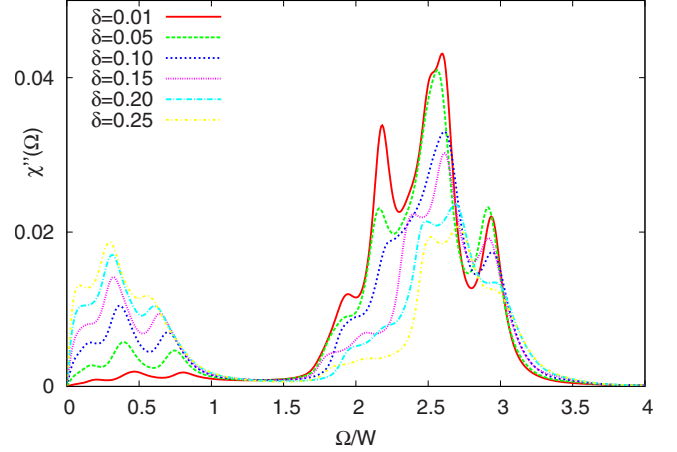


FIG. 1. (Color online) Evolution of the B_{2g} Raman response function for $U/W=2.5$ with doping ranging from $\delta=0.01$ to $\delta=0.25$. The low-energy feature increase in weight for increasing doping, the high-energy one decreases.

Let's first focus on the strong coupling case. Indeed, this correspond to a doped Mott insulator, the critical U at half filling for the chosen density of states (see below) being $U_c/W \approx 1.5$, and at $U/W=3$ the Hubbard bands being split apart by a gap $\Delta \approx 1.5W$.²³

In Fig. 1 we show how the response function calculated in DMFT shows two principal features. These are expected when $\Delta > W$ from the general features of $A(\epsilon, \omega)$ and the smooth form of $V(\epsilon)$.

At zero temperature the Raman response formula simplifies further in;

$$\chi''(\Omega) = \int d\epsilon V(\epsilon) \int_{-\Omega}^0 d\omega A(\epsilon, \omega) A(\epsilon, \omega + \Omega). \quad (23)$$

The integral will be nonzero when, for some ϵ , the two spectral functions shifted by Ω from one another have an overlap in the region $[-\Omega, 0]$, i.e., between the two quasiparticle resonances.

Hence, at low Ω , χ'' will show contributions from the overlap of the two functions within the same Hubbard band, the one in which the quasiparticle peak lies.

At higher $\Omega \gtrsim W$, since the width of the Hubbard band is $\sim W$, if the gap is bigger than the bandwidth ($\Delta > W$), the two spectral functions will have negligible overlap. Indeed, the Hubbard band of one will fall onto the gap of the other and the response will be nearly zero. Then, for even bigger Ω the two spectral functions will be shifted enough so to have the upper Hubbard band of one overlapping the lower Hubbard band of the other. A finite response is found, thus, generating a second well separated feature at these higher frequencies.

If instead $\Delta < W$, this separation of the response will in general not occur.

The evolution of this response function with doping is such that the lower energy feature grows with increasing doping while the higher energy one decreases. This is expected since upon doping the system dilutes and becomes

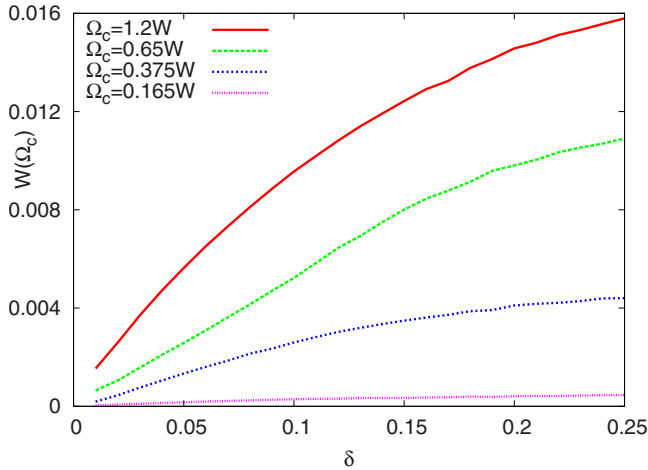


FIG. 2. (Color online) Integrated spectral weight up to a cutoff $\Omega_c = 1.2W$, which fully includes the lower energy feature, of the first moment of the Raman response function plotted versus doping. As predicted for the t - J model $W(\delta) \propto \delta$. Integral up to lower cutoffs are also plotted.

less and less correlated thus causing a transfer of spectral weight back from high to low frequencies.

Physically the separation of the response function into two features means that the Coulomb repulsion is large enough to separate, in energy, the particle-hole excitations happening in the Hubbard band of empty sites from the ones involving doubly occupied sites.

In the strong coupling limit and at low doping, this model can be mapped on a t - t' - J model and this allows us to identify the low-frequency response with that of the t - J model so that we can use it to confirm our analysis on the sum-rule integral.

We thus consider the response under a cutoff $\Omega_c \sim W$ that includes only the processes of the low-energy feature of the Raman response function, namely,

$$W(\Omega_c) \equiv \int_0^{\Omega_c} d\Omega \Omega \chi''_{\text{Hub}}(\Omega) \approx \int_0^{\infty} d\Omega \Omega \chi''_{tJ}(\Omega), \text{ if } \Omega_c \gtrsim W. \quad (24)$$

In Fig. 2 we plot the calculated $W(\Omega_c)$ as a function of different cut-off frequencies Ω_c . The highest value $\Omega_c = 1.2W$ fully includes the low-energy feature of the Raman response in our case, thus reproducing the t - t' - J model sum-rule.

It appears that the linearity in doping of $W(\Omega_c \approx W)$ holds well up to dopings of about 10%, then higher order terms start contributing considerably.

By reducing the cut-off frequency one can see that the integral is still linear in doping. This is somehow expected since the whole lower feature scales with doping and vanishes as the insulating phase is reached for $\delta=0$. The linearity region actually increases and extends up to 15% doping (i.e., the whole underdoped region in cuprates).

The smaller extent of the linear region for the higher cut-offs is probably due to the proximity of the high-energy feature in the response function, which would indeed be com-

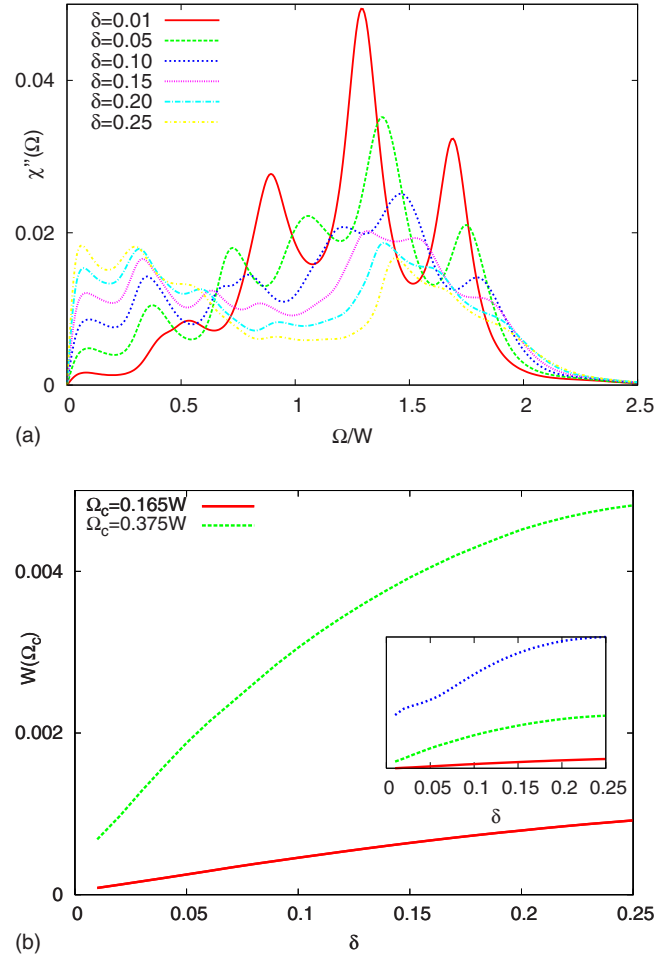


FIG. 3. (Color online) Upper panel: nonresonant B_{2g} Raman response function for $U/W = 1.35 < U_{c2}$. Different curves are, from bottom to top, for increasing dopings $\delta = 0.01 \div 0.25$. The two separate features present at large U/D have now partially merged but the curves still scale with doping at low frequency. Lower Panel: sum-rule integral for cutoffs $\Omega_c = 0.165W$ (lower curve) and $\Omega_c = 0.375W$ (upper curve) for all the chosen cutoffs in Fig. 2: from bottom to top $\Omega_c/W = 0.165, 0.375, 0.65,$ and 1.2 . An intercept is clearly non-negligible for $\Omega_c = 0.65W$, the behavior is no more linear for $\Omega_c = 1.2W$ of the order of the bandwidth.

pletely absent if we were to take the actual $U/W \rightarrow \infty$ limit.

However, in fact, considering a cutoff lower than $\Omega_c \approx W$ is actually directly relevant to the analysis of experimental data on cuprates, as we will see in Sec. V.

Let's now consider the intermediate coupling case.

We studied the model at $U = 1.35W = 0.9U_{c2}$ and obtained the results plotted in the upper panel of Fig. 3. One immediately sees that the two features of the strong coupling case have now merged as the separation of the two Hubbard bands is less than W .

Nevertheless, the low-energy part of $\chi''(\Omega)$ still scales with doping.

In the lower panel of Fig. 3 we plot the value of the integral $W(\Omega_c)$ for small cutoffs as a function of doping. Although the intercept is indeed nonzero, owing to the fact that a quasiparticle resonance is still present at half filling in

this case (which testifies the metallic behavior at half filling that one obtains when U is smaller than the Mott transition critical value U_{c2}), this intercept is practically negligible for the lower cutoffs, given the very little weight of the quasi-particle resonance very close to U_{c2} . Thus, the behavior of the sum-rule integral for small cutoffs is still $\approx \delta$ in the underdoped region for $U \approx 0.9U_{c2}$.

Indeed, by raising the cutoff to values closer to the bandwidth, one eventually loses the linear behavior, owing to the presence of the low-frequency tail of the spectrum of transitions between the two Hubbard bands.

V. CONNECTION WITH EXPERIMENTS: CUT-OFF FREQUENCY AND COUPLING STRENGTH

Some experimental setups are believed to give measures that are accurate enough to extract reliably absolute scattering intensities. We have compiled and analyzed experimental data from two such references,^{24,25} which are shown in Fig. 4. The linear dependence of the absolute intensities in the underdoped region (at least up to $\sim 10\%$ doping) is clearly visible for small cutoffs, up roughly to $2000 \text{ cm}^{-1} \sim 0.25 \text{ eV}$.

Hence, if the experimental cutoff is as low as $\Omega_c \leq 2000 \text{ cm}^{-1} \sim 0.25 \text{ eV}$, Raman spectra can indeed be normalized using a linear scaling in doping, as was done in Ref. 9.

By raising the cutoff around $4000 \text{ cm}^{-1} \sim 0.5 \text{ eV}$, one finds a nonvanishing intercept as is visible in Fig. 4.

It is also very interesting to notice the nonvanishing intercept found for higher cutoffs. This is consistent with the very recent analogous findings of Comanac *et al.* in Ref. 26, where by analyzing optical conductivities of a wide range of cuprates the midinfrared spectral weight ($\Omega_c = 0.8 \text{ eV}$) is found to be nonvanishing despite a vanishing Drude spectral weight ($\Omega_c = 0.2 \text{ eV}$). To explain these experiments, these authors propose to model the optical conductivity of cuprates with a Hubbard model whose interaction strength is less than the single-site DMFT $U_{c2} \approx 1.5W$. This is the value at which a pure Mott transition takes place without additional effects due to magnetic correlations.

Indeed, the calculation we performed in Sec. IV, at $U = 1.35W < U_{c2}$, reproduces the behavior found in the experiments we reviewed. As is clear in the lower panel of Fig. 3, while for intermediate cutoffs, an intercept is sizeable, for the lower cutoffs it is instead very small. Moreover, the antiferromagnetic correlations neglected in this single-site DMFT approach are likely to depress the low-frequency data, thus further reducing the intercept.

There are two possible interpretations of this observation of a finite intercept for the higher values of the cutoff (keeping in mind however that the Raman data used here are taken at slightly different temperatures and that more data are needed).

The first one is that cuprates are actually in the regime of intermediate correlation strength, as recently advocated by Comanac *et al.*²⁶ on the basis of a similar observation from optics. Another possible interpretation of the nonvanishing intercept found for $\Omega_c = 4000 \text{ cm}^{-1}$ are additional contribu-

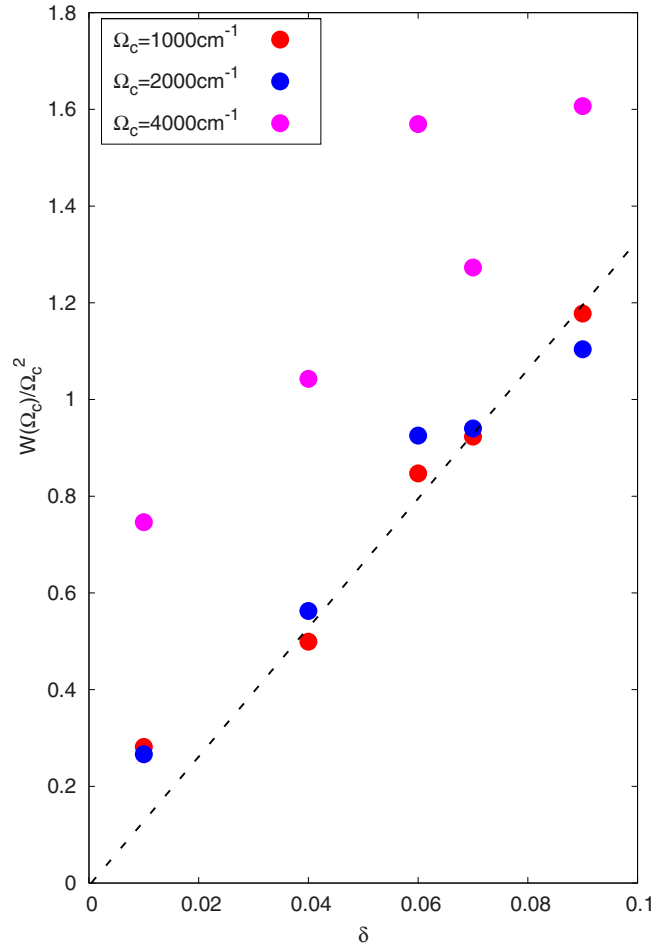


FIG. 4. (Color online) Sum-rule integral $W(\Omega_c)$ calculated from the experimental data on $(Y_{1-y}Ca_y)Ba_2Cu_3O_{6+x}$ in the normal phase, taken from Refs. (17) and (18) here absolute intensities of Raman scattering have been measured. The plots are rescaled by normalizing to the square of the cutoff frequency. The sum-rule linearity holds clearly up to $\delta \sim 0.1$ for both lower cutoffs. The line is a least-square fit of the $\Omega_c = 1000 \text{ cm}^{-1}$ data points, discarding the $\delta = 0.01$ point that corresponds to the antiferromagnetic phase. The curves for these lower cutoffs extrapolate linearly to zero or to a very small intercept. The curve obtained for $\Omega_c = 4000 \text{ cm}^{-1} \sim 0.5 \text{ eV}$ instead does not seem to extrapolate to zero. As discussed in the text, this may indicate either that cuprates are in an intermediate coupling regime (Ref. 26), or that additional magnetic contributions (e.g., two magnons) contribute to the Raman signal in that frequency range.

tions to the Raman scattering of spin origin, such as two magnon processes. To settle this issue clearly, further work is needed.

VI. B_{2g} SUM-RULE IN THE SUPERCONDUCTING PHASE OF THE $t-t'-J$ MODEL: SLAVE BOSONS

In this paragraph we calculate explicitly the right-hand side of Eq. (8) by averaging the calculated expressions for the commutators [Eqs. (14) and (17)] in the slave-bosons mean-field formalism of Ref. 27 used in the early studies of high- T_c 's, which is the simplest approximation that allows to

access the d -wave superconducting phase of the t - t' - J model beside the normal phase.

We recall here briefly this approach. The Hamiltonian of the t - t' - J model [Eq. (9)] lives in the restricted Hilbert space in which all states with a doubly occupied site are projected out. This can be expressed by means of a mixed fermion-boson Hamiltonian,

$$H = \sum_{i,j,\sigma} (t_{ij} f_{i\sigma}^\dagger b_i b_j^\dagger f_{j\sigma} + \text{H.c.}) - \mu \sum_{i\sigma} f_{i\sigma}^\dagger f_{i\sigma} + \sum_{ij} 4J_{ij} \left[(S_i \cdot S_j) - \frac{1}{4} (1 - b_i^\dagger b_i)(1 - b_j^\dagger b_j) \right] + \sum_i \lambda_i \left(\sum_{\sigma} f_{i\sigma}^\dagger f_{i\sigma} + b_i^\dagger b_i - 1 \right), \quad (25)$$

in which the boson operators b_i^\dagger (b_i) represent the creation (destruction) of a hole on-site i , and thus carry the charge degrees of freedom while the pseudofermions $f_{i\sigma}^\dagger$ ($f_{i\sigma}$) carry the spin information. This Hamiltonian lives in the *enlarged* Hilbert space represented by all the possible states of the bosonic and pseudofermionic fields. To complete the mapping, a constraint has to be introduced in order to restrict again this Hilbert space to the physical one by excluding all the nonphysical states. In doing this, one can also implement the non-double-occupancy condition, using namely,

$$\sum_{\sigma} f_{i\sigma}^\dagger f_{i\sigma} + b_i^\dagger b_i = 1. \quad (26)$$

This is expressed in Eq. (25) by means of the Lagrange multipliers λ_i , which enforce the condition on every site.

One then performs a Hartree–Fock–Bogoliubov decoupling and a static mean field (such that $\lambda_i = \lambda$ and the constraint is satisfied on the average, i.e., $\langle b_i^\dagger b_i \rangle = 1 - \sum_{\sigma} \langle f_{i\sigma}^\dagger f_{i\sigma} \rangle = \delta$) on this Hamiltonian by introducing the following mean-field parameters:

$$K = 3J \langle \sum_{\sigma} f_{i\sigma}^\dagger f_{i+x,\sigma} \rangle / 2,$$

$$\Delta_x = -\Delta_y \equiv \Delta = 3J \langle f_{i\uparrow} f_{i+x,\downarrow} - f_{i\downarrow} f_{i+x,\uparrow} \rangle / 2,$$

$$\langle b_i^\dagger b_j \rangle = |\langle b_i \rangle|^2 = 1 - \sum_{\sigma} \langle f_{i\sigma}^\dagger f_{i\sigma} \rangle = \delta. \quad (27)$$

We choose the phase in which K is isotropic (i.e., $K_x = K_y \equiv K$) while the superconducting order parameter has a d -wave symmetry ($\Delta_x = -\Delta_y$). This has been shown to be the actual ground state at finite doping between all the possible symmetries in this kind of mean field.²⁷

The obtained mean-field Hamiltonian reads,

$$H_{\text{MF}} = \sum_{\mathbf{k}\sigma} \epsilon_{\mathbf{k}} f_{\mathbf{k}\sigma}^\dagger f_{\mathbf{k}\sigma} + \left(\sum_{\mathbf{k}\sigma} \Delta_{\mathbf{k}} f_{\mathbf{k}\uparrow}^\dagger f_{-\mathbf{k}\downarrow}^\dagger + \text{H.c.} \right), \quad (28)$$

where

$$\epsilon_{\mathbf{k}} = -2(\delta t - K)(\cos k_x + \cos k_y) + 4\delta t' \cos k_x \cos k_y, \quad (29)$$

$$\Delta_{\mathbf{k}} = 2\Delta(\cos k_x - \cos k_y). \quad (30)$$

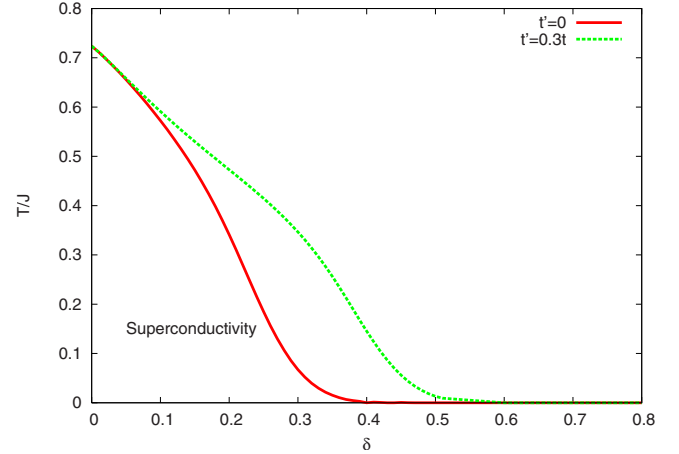


FIG. 5. (Color online) Doping-temperature phase diagram of the t - t' - J model within the Kotliar–Liu slave-bosons mean-field approximation for $J=0.1$ t and $t'=0$ and $t'=0.3$ t . The actual superconducting region is below a condensation temperature of the bosons, where phase coherence sets in. This temperature is an increasing function of doping, so that the superconducting region is dome-shaped. (Ref. 27)

Equations (27)–(30) are the mean-field equations that have to be iterated until a self-consistent solution is found.

The Hamiltonian Eq. (28) is of the standard Bogoliubov bilinear form, and thus, it is trivially solvable (by means of a Bogoliubov substitution). One can then calculate any fermionic average by means of a Wick factorization in terms of the bilinear averages,

$$\langle f_{i\sigma}^\dagger f_{j\sigma} \rangle = \sum_{\mathbf{k}} \cos(\mathbf{k} \cdot \mathbf{r}_{ij}) \langle f_{\mathbf{k}\sigma}^\dagger f_{\mathbf{k}\sigma} \rangle,$$

$$\langle f_{i\sigma}^\dagger f_{j\bar{\sigma}} \rangle = \sum_{\mathbf{k}} \cos(\mathbf{k} \cdot \mathbf{r}_{ij}) \langle f_{\mathbf{k}\sigma}^\dagger f_{-\mathbf{k}\bar{\sigma}} \rangle. \quad (31)$$

This mean-field Hamiltonian of the t - t' - J model has the phase diagram shown in Fig. 5 for $t=10$ J and for $t'=0$ (Kotliar–Liu result) and $t'=0.3t$ (the value generally used for high- T_c superconductors like BiSCCO).

For each doping there are two phases, a low-temperature (superconducting) phase with $\Delta \neq 0$ and a high-temperature (normal) phase with $\Delta=0$. The transition temperature is denoted T_{RVB} and is a decreasing function of doping. The bosons are treated here as fully condensed because $\langle b_i^\dagger b_i \rangle = |\langle b_i \rangle|^2 = \delta$ at all temperatures.

If we were to allow bosons decondensation (which requires to include the link variational parameter $\langle b_i^\dagger b_j \rangle$ as well), another crossover temperature (zero at half filling and rapidly increasing with doping) would delimit a low-temperature phase with phase coherence from the disordered phase of incoherent pairs. The actual superconducting region has a domelike structure centered around a region of “optimal” doping where the two characteristic temperatures cross.

In this formalism it is then possible to calculate the right-hand side of Eq. (8) by taking each Hubbard operator product in the two parts of the commutators [Eqs. (14) and (17)] and obtain the expression in terms of the f s and the b s using

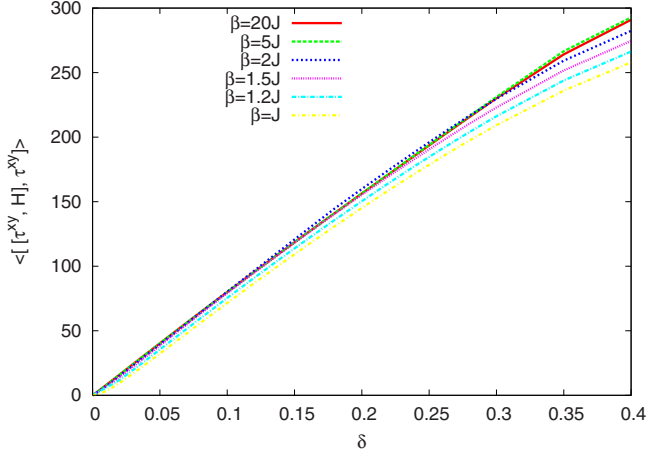


FIG. 6. (Color online) Right-hand side of the sum-rule evaluated in the t - t' - J model within the Kotliar–Liu slave-bosons mean-field approximation for different temperatures and parameters $J=0.1t$ and $t'=0.3t$. The bottom curve is calculated for $\beta=J$, entirely in the normal phase, and shows how the linearity holds pretty well also for the normal phase in the whole range of dopings.

Eq. (15). Then one performs the Wick factorization of each product [i.e., following the example of Eq. (16)]. One obtains $\langle f_{a\alpha}^\dagger f_{a\alpha} f_{b\sigma}^\dagger f_{b\sigma} \rangle = \langle f_{a\alpha}^\dagger f_{a\alpha} \rangle \langle f_{b\sigma}^\dagger f_{b\sigma} \rangle - \langle f_{a\alpha}^\dagger f_{b\sigma} \rangle \langle f_{b\sigma}^\dagger f_{a\alpha} \rangle - \langle f_{a\alpha}^\dagger f_{b\sigma} \rangle \langle f_{a\alpha} f_{b\sigma} \rangle$, and by means of the bilinear averages Eq. (31) calculated with H_{MF} within the converged solution one obtains the final result. This result is plotted in Fig. 6 as a function of doping at different temperatures.

The results show that in the superconducting phase at $T < T_{RVB}$ the sum-rule integral is linear in doping until 30–40% doping, thus, allowing the linear scaling of the Raman spectra in doping for the full extent of the superconducting phase of cuprates.

Still, one has to be aware of the many limitations of this simple mean field. Beside the cited boson decondensation, which adds a second energy scale to the problem, less relevant to our analysis, the method lacks a second *fermionic* energy scale that is new and very debated point put forward in Ref. 9. Our analysis in terms of the Kotliar–Liu slave bosons has to be taken, thus as a qualitative description of the nodal physics in the superconducting phase.

It is also interesting to plot the temperature dependence of the sum-rule integral.

In order to compare the temperature dependence in the superconductive phase at different dopings, in Fig. 7 we plot $\langle [[\tau^{xy}, H], \tau^{xy}] \rangle / \delta$, owing to the doping linearity. The rescaled curves indeed lie all in the same range of values but show a different behavior in temperature depending on the doping value. While at low doping raising, the temperature causes a decrease in the sum-rule value, after $\delta \sim 12\%$ (which could be interpreted as “optimal doping” in this slave-bosons mean-field) the value instead increases with increasing temperatures. Then, in general when the system enters the normal phase upon heating, the integral value shows a cusp and then drops quickly.

This behavior has not yet been measured and it is a prediction of this slave-boson mean-field treatment that would be very interesting to clarify in further experiments.

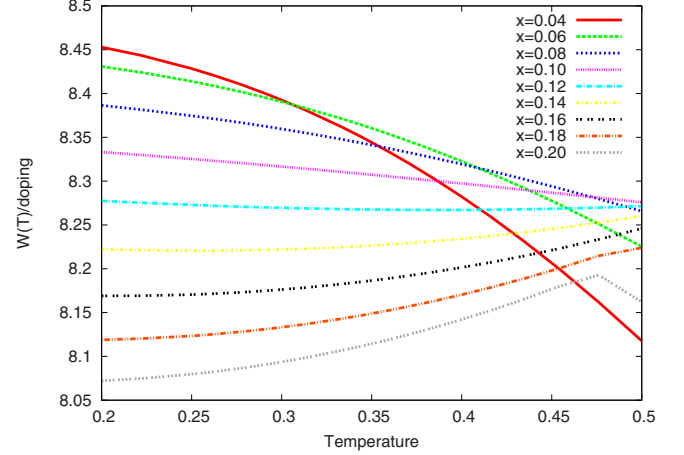


FIG. 7. (Color online) Temperature dependence of the sum-rule in the slave-bosons formalism in the superconducting phase. For increasing temperature the integral decreases at low doping while it increases at higher doping.

VII. CONCLUSIONS

We have studied a restricted sum-rule for Raman scattering, which involves the first moment of the nonresonant B_{2g} response function up to a cut-off frequency: $\int_0^{\Omega_c} d\Omega \Omega \chi''_{B_{2g}}(\Omega)$.

For the doped t - t' - J model, where we can take the cutoff $\Omega_c = \infty$, we have shown that this integral is proportional to the doping level. This supports the experimental data analysis of Ref. 9.

We have then calculated the Raman response function and studied its doping dependence for the normal phase of the Hubbard model within DMFT.

We have first studied the system in the strong coupling case $U=2.5W$, which corresponds to a doped Mott insulator. In this case the low-frequency response of this system can be identified with the one of the t - t' - J model and we have confirmed its linearity in doping at low doping.

We have then studied the intermediate coupling case $U=1.35W=0.9U_{c2}$, showing that in this case the sum-rule integral still shows a behavior $\approx \delta$ for very low cutoffs, while the intercept is non-negligible for intermediate cutoffs.

We have also shown a compilation of experimental data that are believed to correctly measure the absolute intensity of Raman scattering on YBCO. As in our DMFT study at $U=1.35W$, the behavior is $\approx \delta$ at low cutoffs ($\Omega_c \lesssim 0.125$ eV) but shows a non-negligible intercept already for $\Omega_c \sim 0.25$ eV. This can be interpreted in support of the hypothesis that cuprates are “intermediately correlated” as recently put forward in Ref. 26.

Finally we have studied the superconductive phase of the t - t' - J model using the slave-boson method of Ref. 27. We can calculate explicitly the right-hand side of the sum-rule in this approximation and we show its linearity in doping up to dopings of order of 30% and a prediction on the temperature dependence.

The combination of those results gives a first indication on how the strong correlations affect integrated Raman intensities. Missing at this point, a systematic study of the

effect of dynamical short-range magnetic correlations since the slave-boson method captures these in a primitive fashion using static link expectation values. These limitations can be removed using cluster versions of dynamical mean-field theory²⁸ and this is left for future studies.

ACKNOWLEDGMENTS

L.d.M. thanks A. Camjayi, L. De Leo, and M. Capone for useful discussions. A.G. and G.K. acknowledge an earlier collaboration and discussions with A. Sacuto and M. Le Tacon, as well as the discussions with N. Bontemps. This work was supported by the NSF under Grant No. DMR 0528969 and by the Blaise Pascal Chair.

APPENDIX: SOME ALGEBRA OF THE HUBBARD OPERATORS USED IN THIS PAPER

Hubbard operators on-site i are defined as

$$X_{\alpha\beta}^i = |\alpha\rangle_i \langle\beta|_i; \quad |\alpha\rangle, |\beta\rangle = |0\rangle, |\uparrow\rangle, |\downarrow\rangle, \quad (\text{A1})$$

and hence, they are used to enforce the constraint of no on-site double occupancy since they all project the $|\uparrow\downarrow\rangle$ state to zero.

From their definitions it is easy to show that two Hubbard operators acting on the same site observe the following commutation (anticommutation) relations:

$$[X_{\alpha\beta}^i, X_{\gamma\delta}^i]_{\pm} = \delta_{\beta\gamma} X_{\alpha\delta}^i \pm \delta_{\alpha\delta} X_{\gamma\beta}^i. \quad (\text{A2})$$

Instead, two operators acting on different sites respect the canonical commutation or anticommutation relations depending on them being “fermionic” ($X_{0\sigma}$ or $X_{\sigma 0}$ that add or remove a spin-1/2) or “bosonic” ($X_{00}, X_{\sigma\sigma'}$ that either don’t change the onsite spin or they add or remove a spin 1), i.e.,

$$[X_B^i, X_B^j] = 0, [X_F^i, X_F^j]_{\pm} = 0, [X_B^i, X_F^j]_{\pm} = 0, \quad \forall i \neq j, \quad (\text{A3})$$

where “B” is for bosonic and “F” is for fermionic. Indeed these operators are not actual bosons or fermions since on site they respect the (A2).

It is useful in our calculations to introduce the bosonic operator $D_{\alpha\beta}^i$ corresponding to the particular case of (A2) for the onsite anticommutation of two fermionic operators;

$$[X_{\alpha 0}^i, X_{0\beta}^i]_{\pm} = X_{\alpha\beta}^i + \delta_{\alpha\beta} X_{00}^i \equiv D_{\alpha\beta}^i. \quad (\text{A4})$$

and also its on-site commutation relations with the others Hubbard operators;

$$[D_{\sigma\sigma'}^i, X_{\alpha\beta}^i]_{\pm} = \delta_{\sigma'\alpha} X_{\sigma\beta}^i - \delta_{\sigma\beta} X_{\alpha\sigma'}^i + \delta_{\sigma'}(\delta_{\alpha 0} X_{0\beta}^i - \delta_{\beta 0} X_{\alpha 0}^i). \quad (\text{A5})$$

-
- ¹R. Kubo, J. Phys. Soc. Jpn. **12**, 570 (1957).
²M. R. Norman and C. Pepin, Phys. Rev. B **66**, 100506(R) (2002).
³A. Millis, in *Strong Interactions in Low Dimensions*, edited by D. Baeriswyl and L. Degiorgi (Springer-Verlag, Berlin, 2004).
⁴D. van der Marel, *Strong Interactions in Low Dimensions* (Ref. 3).
⁵G. Deutscher, A.-F. Santander-Syro, and N. Bontemps, Phys. Rev. B **72**, 092504 (2005), and references therein.
⁶J. Kosztin and A. Zawadowski, Solid State Commun. **78**, 1029 (1991).
⁷J. K. Freericks, T. P. Devereaux, M. Moraghebi, and S. L. Cooper, Phys. Rev. Lett. **94**, 216401 (2005).
⁸B. S. Shastry and B. I. Shraiman, Phys. Rev. Lett. **65**, 1068 (1990).
⁹M. Le Tacon, A. Sacuto, A. Georges, G. Kotliar, Y. Gallais, D. Colson, and A. Forget, Nat. Phys. **2**, 537 (2006).
¹⁰A. J. Millis, Science **314**, 1888 (2006).
¹¹W. Guyard, M. LeTacon, M. Cazayous, A. Sacuto, A. Georges, D. Colson, and A. Forget, Phys. Rev. B **77**, 024524 (2008).
¹²A. V. Chubukov and M. Norman, arXiv:0802.4241, Phys. Rev. B (to be published).
¹³W. Guyard, A. Sacuto, M. Cazayous, Y. Gallais, M. L. Tacon, D. Colson, and A. Forget, arXiv:0802.3166 (unpublished).
¹⁴T. Devereaux and R. Hackl, Rev. Mod. Phys. **79**, 175 (2007), and references therein.
¹⁵G. Mahan, *Many-Particle Physics* (Plenum, New York, 1981).
¹⁶Using the spectral representation, one can also show that the relation $\frac{2}{\pi} \int_0^{\infty} d\Omega \frac{\chi_{\mathcal{O}\mathcal{O}}^{\prime}(\Omega)}{\Omega} = \chi'_{\mathcal{O}\mathcal{O}}(0)$ holds as a sum-rule for any sus-

ceptibility, which is also trivially an outcome of the Kramers–Kronig relations. Hence, another sum-rule holds for the nonresonant Raman response: $\frac{2}{\pi} \int_0^{\infty} d\Omega \frac{\chi_{\tau^x\tau^y}^{\prime}(\Omega)}{\Omega} = \chi'_{\tau^x\tau^y}(0)$. It is worth noting that contrary to the sum-rule studied in the main text Eq. (8), this one is related (Ref. 8) to the optical sum-rule for the conductivity $\sigma(\omega)$ [i.e. $\omega\sigma'(\omega) \propto \chi''(\omega)$] and hence is expected to stem out of a conservation law as it is for the latter (conservation of the charge). The sum-rule Eq. (8), instead, does not come from a conservation law and this makes its integral up to a bandwidth more sensible to the temperature and the phase, as studied in Sec. VI.

- ¹⁷Note that the diagonal terms of the Hamiltonian—e.g., the chemical potential term—commute with the stress operator, hence, they do not contribute to the sum-rule. We will consider $t_{ii}=0$ from now on.
¹⁸When averaged, an X_{00} operator leads a renormalization factor $\propto \delta$, unless if it shares the site index with other operators in the product in which case it has to be simplified as in Eq. (16). In the expression under examination it is never the case since when $a, d=b$ the coefficient vanishes given the presence of $\tau_{ab}\tau_{bd}$.
¹⁹A. Georges, G. Kotliar, W. Krauth, and M. J. Rozenberg, Rev. Mod. Phys. **68**, 13 (1996).
²⁰We are interested here in the Raman response of a bidimensional cubic lattice, so in the calculation of the response function we will make use of a form factor obtained by integrating functions of the cubic dispersion [Eq. (5)] over the bidimensional Brillouin zone. Hence, DMFT here has to be thought as a local self-energy approximation of the finite dimensional lattice rather than the solution of the ∞ -dimensional counterpart of the model

under investigation. In this light the choice of a semicircular DOS (see the footnote on DMFT technical data) for the impurity model (which facilitates the numerical solution) is not a severe inconsistency with the cubic dispersion used in the response function.

²¹The Anderson impurity model associated with DMFT to the Hubbard model has been solved by means of the exact diagonalization of the Hamiltonian. The impurity model Hamiltonian has been limited to eight sites (impurity +7 sites in the effective bath), and it has been diagonalized at zero temperature by means of the Lanczos algorithm. The projection of the Anderson bath on the limited subspace is obtained by means of a best fit on a grid of frequencies on the imaginary axis, corresponding to a fictive temperature of $\beta=500$ and slightly weighted towards low frequencies. The DOS entering the bath self-consistency condition is semicircular, of bandwidth W . The self-energy obtained from the impurity model with this choice of the density of states (DOS) equals the self-energy of an infinite dimensional Bethe lattice.

²²The real-axis self-energies are calculated for $\omega=\omega+i\Gamma_{br}$, with $\Gamma_{br}=0.1$ in order to smoothen out the spikes due to the discretization of the bath.

²³The spectral function $A(\epsilon, \omega)$ of the doped Hubbard model has a well-known three-peak structure (Ref. 19) formed by a resonance peak close to the chemical potential (in the metallic phase) and two features lying, at an energy $\sim U$ from one another in the ‘‘Hubbard bands.’’ This two energy intervals are of width W and are separated by a gap $\Delta \sim U - W$. In the doped phase the chemical potential lies within one of them.

²⁴M. Opel *et al.*, Phys. Rev. B **61**, 9752 (2000).

²⁵L. Tassini, W. Prestel, A. Erb, M. Lambacher, and R. Hackl, arXiv:0705.3635 (unpublished).

²⁶A. Comanac, L. de’Medici, M. Capone, and A. Millis, Nat. Phys. **4**, 287 (2008).

²⁷G. Kotliar and J. Liu, Phys. Rev. B **38**, 5142(R) (1988).

²⁸G. Biroli, O. Parcollet, and G. Kotliar, Phys. Rev. B **69**, 205108 (2004).